HHS Public Access

Author manuscript

Ann N Y Acad Sci. Author manuscript; available in PMC 2020 April 01.

Published in final edited form as:

Ann N Y Acad Sci. 2019 April ; 1442(1): 91–103. doi:10.1111/nyas.13991.

Retention of osteocytic micromorphology by sclerostin antibody in a concurrent ovariectomy and functional disuse model

Dongye Zhang[1], **Marianna Miranda**[1], **Xiaofei Li**[1], **Jiangmeng Han**[1], **Yueli Sun**[1], **Nancy Rojas**[1], **Shan He**[2], **Minyi Hu**[1], **Liangjun Lin**[1], **Xiaodong Li**[3], **Hua Zhu Ke**[4], and **Yi-Xian Qin**[1]

[1]Dept. of Biomedical Engineering, Stony Brook University, Stony Brook, NY

[2]Dept. of Material Science Engineering, Stony Brook University, Stony Brook, NY

[3]Dept. of Metabolic Disorders, Amgen, Inc., Thousand Oaks, CA

[4]UCB Pharma, Slough, UK

Abstract

Prolonged mechanical unloading in bed-ridden patients and concurrent hormonal dysregulation represents the cause of one of the most severe forms of osteoporosis, a condition for which there are very few efficacious interventions available to date. Sclerostin, a Wnt antagonist, acts as a negative regulator of bone formation. Sclerostin antibody–mediated blockade of sclerostin can dramatically enhance bone formation and reduce bone resorption. This study was designed to investigate the therapeutic effect of the sclerostin antibody (Scl-Ab) on severe bone loss induced by concurrent mechanical unloading and estrogen deficiency in a hindlimb-suspended and ovariectomized rat model, and to study the cellular mechanisms underlying severe osteoporosis and Scl-Ab action. Unloading and ovariectomy resulted in severe loss of trabecular and cortical bone mass and strength; Scl-Ab can significantly counteract the deterioration of bone in unloaded and/or ovariectomized rats, with noticeably increased cortical bone formation. Scanning electron microscopy analysis revealed that unloading and ovariectomy lead to multiple morphological and structural abnormalities of osteocytes in cortical bone and the abnormalities were abolished by Scl-Ab administration. This study extends our previous conclusion that Scl-Ab represents a promising therapeutic approach for the severe bone loss that occurs after being exposed to estrogen deficiency and prolonged mechanical unloading.

Graphical abstract

Corresponding Author: Yi-Xian Qin, Ph.D., Address: Dept. of Biomedical Engineering, State University of New York at Stony Brook, 215 Bioengineering Bldg., Stony Brook, NY 11794-5281, yi-xian.qin@stonybrook.edu.

Authors' Contributions: This study was conceived by YXQ and HZK. MH performed part of the animal study jointly with DZ. DZ and MM were responsible for cortical bone histomorphometry sectioning, contouring, and analysis. LL helped with the MTS system setting. DZ performed animal studies, extraction of tissue samples, μCT analysis, histomorphometry analysis, mechanical bending test, immunoassay analysis, and SEM analysis. NR, SH, XL, JH, and YS assisted in the SEM analysis. Data were analyzed and interpreted by DZ, XL, JH, and YS. The draft manuscript was written by DZ and revised by each author, particularly by MH, XL, and YXQ. The final draft of the manuscript was approved by YXQ.

Competing Interests

Xiaodong Li is an employee of Amgen, Inc. Hua Zhu Ke is an employee of UCB Pharma. This project was partially sponsored by Amgen, Inc.

This paper investigates the therapeutic effect of the sclerostin antibody on severe bone loss induced by concurrent mechanical unloading and estrogen deficiency in a hindlimb-suspended and ovariectomized rat model, and examines the cellular mechanisms underlying severe osteoporosis and sclerostin antibody action.

Keywords

sclerostin antibody; osteocyte; severe osteoporosis; scanning electron microscopy; mechanical unloading; estrogen deficiency

Introduction

Osteoporosis is a chronic metabolic disease caused by the imbalance between bone formation and bone resorption in the bone remodeling process in which osteoclasts resorb bone tissues while osteoblasts generate and mineralize new bone matrix[1, 2]. With its high prevalence and incidence rate, osteoporosis has been identified as a global healthcare problem, with 44 million people in the United States at risk, leading to a direct annual medical cost of around $20 billion, and this number is expected to grow sharply with the increase of the aged population in the future[3–7]. The proper development and maintenance of bone matrix integrity are coordinated exquisitely by multiple factors, including systemic and local hormones (such as estrogen and parathyroid hormone), cytokines, and mechanical loading[8–10]. Among the risk factors that contributes to the development of osteoporosis in elderly women is estrogen deficiency in post-menopausal women[11]. Mechanical unloading caused by various environmental or pathological conditions, such as immobilization or weightlessness experienced by long-term bed-ridden patients or astronauts, respectively, represents another critical cause of reduced bone integrity and strength[12–15]. Without doubt, the combination of mechanical unloading and estrogen deficiency may exacerbate the condition and contribute to one of the most severe forms of osteoporosis and to greatly increased risk of fractures due to the grave pathophysiological changes caused by immobilization accompanied by estrogen disruption[16].

Sclerostin, a negative regulator of bone formation, is encoded by the *SOST* gene and secreted predominantly by osteocytes[17–23]. It acts to inhibit the Wnt/β-catenin signaling pathway, which regulates bone formation and bone resorption by competing with Wnt for binding to the LRP5/LRP6-Frizzled co-receptors in osteoblast cell membrane, which will lead to a cascade of downstream intracellular changes that in turn regulate osteoblastic bone formation through gene transcription[24–26]. Prolonged mechanical disuse (e.g., hindlimb unloading) has been associated with up-regulation of osteocyte expression of sclerostin[27, 28]. Although the abrupt decline of estrogen that follows menopause or ovariectomy (OVX) surgery has an inconclusive effect on sclerostin levels[29], the impairment of the normal bone remodeling cycle that results in increased osteoclastic resorption activity and uncoupled osteoblastogenesis following estrogen deficiency is well documented[30]. Estrogen deficiency may suppress the secretion of osteoprotegerin (OPG; also known as TNFRSF11B), a decoy receptor for the receptor activator of nuclear factor kappa B ligand (RANKL; also known as TNFSF11), which may strengthen RANKL-RANK interactions that promote the

differentiation of osteoclast precursors into mature osteoclasts[31]. Collectively, mechanical disuse with concurrent estrogen deficiency has the potential to lead to severe loss of bone mass and strength in large part due to the concomitant inhibition of bone formation activities resulting from mechanical unloading and a disproportionate increase of bone resorption activation resulting from both mechanical unloading and estrogen depletion.

It has been demonstrated in previous studies that severe osteoporosis induced by mechanical unloading and concurrent estrogen deficiency leads to dramatic trabecular bone loss and severe microarchitecture deterioration as well as the remarkable decline of bone strength in the femur, which implies a greater chance of fragility fractures. This rapid and profound deterioration of bone tissue has been associated with elevated bone resorption as well as a notable suppression of bone formation[32, 33]. Sclerostin antibody (Scl-Ab) has proven effective in preserving bone mass and strength in this type of osteoporosis. The mechanism by which Scl-Ab exerts its therapeutic effect is thought to be through both improving bone formation and the regulation of bone resorption. However, it remains unclear how osteoporosis induced by both mechanical unloading and estrogen deficiency, and the beneficial effect of Scl-Ab, exerts its influence on osteocytes that subsequently crosstalk with osteoblasts and osteoclasts in the context of bone remodeling. Thus, in this study, we used a rat osteoporosis model that combines both hindlimb unloading as well as ovariectomy to study the potential devastating results of prolonged mechanical unloading combined with estrogen deficiency on cortical bones. The potential therapeutic effect of Scl-Ab in this rat osteoporosis model was also evaluated on cortical bone mass, bone strength, and histomorphometric indices of bone formation. In addition, osteocyte structures and morphologies were also examined by using scanning electron microscopy (SEM) following osteoporosis induction and Scl-Ab treatment, in the hope of shining light on the potential cellular mechanisms for severe osteoporosis and the therapeutic effect of Scl-Ab as a promising new intervention.

Materials and Methods

Animals, Scl-Ab administration, and tissue harvesting

All experimental procedures and animal models described below had been approved by the Institutional Animal Care and Use Committee (IACUC) at Stony Brook University. A total of 77 four month–old female Sprague Dawley rats were purchased from Charles River Laboratory (Wilmington, MA) for this study. All rats underwent either sham or OVX surgeries, and they were allowed two weeks of recovery before the study. Upon their arrival at the Stony Brook University Division of Laboratory Animal Resources (DLAR), where they were housed individually in a temperature-controlled environment with a 12:12 hour light:dark cycle, the rats weighed an average of 327 ± 25 g. They were subjected to either functional disuse or free ambulation after two days of quarantine and acclimation. Functional disuse was carried out by the hindlimb suspension (HLS) technique, where a tail harness device was attached to the tail of the rats that had been cleaned with 70% isopropyl ethanol and coated with a thin layer of benzoin. A swivel apparatus was attached to the other end of the tail harness device and suspended from the roof of the cage[34]. The animals were maintained at an approximately 30° head-down tilt to to make sure that their hindlimbs were

prevented from touching the floor of the cage at all times during the experiment, while the forelimbs were allowed free movement. Animals were divided into seven groups, with n = 10–11 per group: (1) Sham + Veh (vehicle), (2) Sham + HLS + Veh, (3) Sham + HLS + Scl-Ab, (4) OVX + Veh, (5) OVX + Scl-Ab, (6) OVX + HLS + Veh, (7) OVX + HLS + Scl-Ab. All groups were subjected to subcutaneous injection of either phosphate-buffered saline (PBS) or Scl-Ab (Amgen, Thousand Oak, CA, USA) at 25 mg/kg twice per week for five weeks starting at the time of HLS[35, 36]. The injection solution was freshly made at the time of injection each time, and the antibody was aliquoted and stored at −80 °C. For histomorphometric labeling, all rats were subjected to two subcutaneous calcein (Sigma-Aldrich Inc., St. Louis, MO, USA) injections (15 mg/kg) at 3 and 13 days before euthanasia. All animals were checked twice a day, and their health was monitored closely throughout the study. At the end of the study, femurs were harvested and subjected to radiological, mechanical, histomorphological and microscopic analysis. Animal euthanization was performed via cervical dislocation under isoflurane inhalation anesthetization after five weeks of the study. Both the right and left tibias and the right and left femurs of animals from all groups were harvested and preserved in 70% EtOH at −20 °C after muscle and connective tissues were carefully removed.

Analysis by μCT

A high-resolution μCT scanner (μCT-40, SCANCO Medical AG, Bassersdorf, Switzerland) was used for scanning the midshaft of femurs with a spatial resolution of 15 μm. Specific Gaussian sigma, support, and lower threshold of 0.5, 1, and 330, respectively, were used for defining analyzed objects and image smoothing purposes. One 3000 μm portion of the midshaft region of the femur was chosen as the area of interest. Cortical bone thickness (Ct.Th.) was evaluated for the trabecular region.

Histomorphometry

Histomorphometry study was performed after μCT scanning and 4-point bending based on previously published protocols[32, 33]. The midshaft portion of the intact femur was dissected using a low-speed diamond wheel saw (South Bay Technology, Inc., San Clemente, CA, USA). The dissected samples (~5mm in length) were dehydrated with isopropanol and then infiltrated and embedded with a mixture of methyl methacrylate (MMA), di-butyl phthalate, and benzoyl peroxide. After the media were cured, the polymethyl methacrylate (PMMA) blocks were sectioned into 5 μm slices using a Leica 2165 microtome (Leica, Wetzlar, Germany). The whole midshaft area was examined as the region of interest using Osteomeasure software (OsteoMetrics Inc., Decatur, GA, USA) to trace the calcein label in the cortical bone under a fluorescent microscope. Femur midshaft static parameters, e.g., cortical thickness (Ct.Th., mm), and dynamic histomorphometric parameters, including endosteal and periosteal mineralizing surface/bone surface (Ec. MS/BS and Ps. MS/BS, %), mineral apposition rate (Ec. MAR and Ps. MAR, μm/day), and bone formation rate (Ec. BFR/BS and Ps. BFR/BS, μm/day × 100), were evaluated.

Scanning electron microscopy (SEM) Analysis

In our previous study, we analyzed femoral trabecular bone histomorphometric changes. A cut was made along the sagittal plane of the right femur, and the medial side was embedded

in PMMA and dissected for this purpose. The same samples were used in this study for the SEM imaging technique. The experimental procedure has been well documented in the published literature[8, 37, 38]. Briefly, the surface of the specimen was acid-etched with 37% phosphoric acid for 10 s and then washed 5 times using distilled water for 2 min each. This was followed by a 5% sodium hypochlorite wash for 10 min. Distilled water was used to wash the samples 5 times for 2 minutes each. The PMMA blocks were then air-dried overnight. The surface of the specimen was coated with gold-palladium for SEM imaging. Cortical bone midshaft osteocyte number per bone area was quantified under 1000× magnification; osteocyte dendrite number and surface area were quantified under 5000× magnification; osteocyte dendrites width is quantified using 10,000× magnification. To characterize the shape parameters of osteocytes, the assumption was made that they are prolate spheroids. The shape of osteocytes was characterized by the ratio of their long axis and short axis and their volume under 2000× magnification. The volume of osteocytes was calculated as $V = \frac{4}{3}\pi ab^2$, where a is the length of the long axis and b is the length of the short axis (Figure 6C). All parameters were quantified using ImageJ.

Statistical Analysis

All results are reported as mean ± SD for all the analyses. Mechanical testing, μCT, histomorphometry, and SEM data were all evaluated using GraphPad Prism software (version 5.01, GraphPad Software Inc., San Diego, CA, USA). One-way analysis of variance (ANOVA) with Tukey's pairwise multiple comparison tests were performed on all data from the femoral mid-diaphysis. Differences between two groups were considered significant at a P value of less than 0.05.

Results

Scl-Ab prevents loss of cortical bone mass and strength

The diaphyseal cortical bone of the midshaft femurs was analyzed with μCT. Ct.Th data revealed that 5 weeks of mechanical unloading alone resulted in 13.7% ($P < 0.05$) loss in cortical thickness compared to the sham control. OVX animals treated with Veh experienced a significant decrease in the cortical thickness of 14.2% ($P < 0.05$), while Veh-treated OVX rats with concurrent HLS resulted in a slightly greater bone loss of 15.4% ($P < 0.05$) as compared to the sham control. Scl-Ab injection was associated with significantly elevated and well-preserved cortical bone thickness in the femur midshaft in all groups administered with Scl-Ab, with an increase of 19.0% ($P < 0.05$), 13.8% ($P < 0.05$) and 15.1% ($P < 0.05$), respectively (Fig. 1).

Scl-Ab greatly induces cortical bone formation

Figure 2 shows representative images of calcein-labeled cortical bone. The data for histomorphometric analysis of midshaft femoral diaphysis cortical bone is presented in Figure 3A-3F. Clear double calcein labeling could be observed at both endosteum and periosteum sites in the HLS alone, OVX alone and HLS + OVX groups that were administered with Scl-Ab for 5 weeks. Without Scl-Ab treatment, this labeling was absent after 5 weeks of mechanical unloading, estrogen deficiency, or both. The Scl-Ab-treated

HLS, OVX and HLS + OVX groups showed a significant increase in the mineral surface as compared to the respective controls at both periosteum (Ps. MS/BS, %) and endosteum (Ec. MS/BS, %) sites, indicating an increased mineralizing surface area versus total bone surface area. Following Scl-Ab administration, the mineral apposition rate at both the periosteum (Ps. MAR, μm/day) and endosteum (Ec. MAR, μm/day) surface only showed a substantial increase in HLS alone animals, although the periosteum bone formation rate (Ps. BFR, μm/day), which is the product of MAR and MS/BS, demonstrated a significant increase of 721% ($P < 0.05$) in the HLS alone group, 55% ($P < 0.05$) in the OVX alone group, and 460% ($P < 0.05$) in the HLS + OVX group. The endosteum bone formation rate (Ec. BFR, μm/day) following Scl-Ab administration similarly showed a significant increase of 636% ($P < 0.05$) in the HLS alone group, 42% ($P < 0.05$) in the OVX alone group, and 312% ($P < 0.05$) in the HLS + OVX group, as compared to the respective controls.

Scl-Ab administration preserves osteocyte morphology and structure

The mechanisms by which osteocytes regulate bone deterioration after the combination of mechanical unloading and estrogen deficiency and by which they preserve cortical bone volume and strength after the administration of Scl-Ab were investigated. The morphology and the number and size of the osteocytes were quantified using SEM (Fig. 4). Representative SEM images of osteocyte and matrices are shown in the Figure 5. The osteocyte number per unit cortical bone area (Ct. Osteocyte #/mm^2) was significantly decreased by ~30% after either HLS, OVX, or the combination of both treatments ($P < 0.01$, $P < 0.001$, and $P < 0.001$, respectively; Fig. 4B). While the reduction of the osteocyte number per cortical bone area with either HLS, OVX, or both treatments was abolished by Scl-Ab treatment for 5 weeks ($P < 0.001$, $P < 0.01$, and $P < 0.001$, respectively; Fig. 4A), the osteocyte surface area (μm^2) was not affected by HLS, OVX, or HLS+OVX treatment, with either Veh or Scl-Ab administration (Fig. 4B). Additionally, osteocyte dendrite number (Dendrite #) was significantly decreased in HLS, OVX and HLS + OVX animals as compared to the sham control ($P < 0.001$, $P < 0.001$, and $P < 0.001$, respectively; Fig.4C), while this reduction was not observed in Scl-Ab-treated animals ($P < 0.001$, $P < 0.01$, and $P < 0.001$, respectively; Fig. 4C). However, there was no significant change of osteocyte dendrite width (nm) among all the groups, regardless of the treatment (Fig. 4D). Additionally, the HLS, OVX, and HLS + OVX groups all had disorganized and poor mineralization as compared to the consistent woven appearance of the control and Scl-Ab-treated groups (Figure 5; white arrows).

The shape of osteocytes was also quantified. The ratio of the long and short axis of the osteocyte was found to increase significantly under the HLS condition with Veh treatment while Scl-Ab significantly reduced the ratio in HLS and OVX alone groups to a level that is lower than the age-matched control group. The ratio in the HLS + OVX group did not change significantly as compared with the age-matched control regardless of the treatment (Fig. 6A). Osteocyte volume did not show significant changes in the HLS control group, while the volume doubled in the OVX and HLS + OVX groups treated with Veh. Scl-Ab increased the volume of osteocytes 3-fold in HLS animals and decreased the volume of osteocytes in OVX animals compared to the age-matched control (Fig. 6B).

Discussion

In this study, we demonstrated for the first time that cortical bone is susceptible to severe osteoporotic deterioration induced by mechanical unloading and estrogen deficiency and can be rescued by Scl-Ab administration, which further emphasizes the notion that Scl-Ab represents a promising anabolic agent with potent effects on bone[8]. We utilized a severe osteoporosis rat model that combines mechanical unloading and concurrent estrogen deficiency and characterized the loss in cortical bone at the tissue and cellular level using SEM. Remarkably, the HLS alone, OVX alone, and HLS + OVX groups are all associated with a significant loss of cortical thickness compared with the age-matched control group. This result is consistent with our previously published study on the effect of the combination of mechanical unloading and estrogen deficiency on trabecular bone, where a severe 87% loss of trabecular bone in distal femur was discovered using μCT[32]. The changes in cancellous bones in terms of bone mass had been reported to be more pronounced than that in cortical bones but mostly follows a similar pattern[39]. Taking these observations together, it becomes clear that severe osteoporosis induced by mechanical unloading and/or an abrupt decline of ovarian production of estrogen in post-menopause females negatively affects long bones in the lower extremities[13, 40–42]. In addition to the significantly decreased cortical bone thickness in this osteoporosis scenario, OVX + HLS rats also demonstrated impaired cortical bone mechanical properties, e.g., stiffness and ultimate load. Strong correlations were observed between μCT-measured Ct.Th. and mechanical testing parameters such as stiffness ($R^2 = 0.8625$) and ultimate load ($R^2 = 0.7081$) (Table 1). Scl-Ab has been studied extensively in recent years and has been recognized as a potent and effective therapeutic bone anabolic agent based on numerous animal studies and clinical trials[43–45]. Scl-Ab was able to completely block the deleterious effect of estrogen deficiency and concurrent mechanical disuse on cortical bone thickness, and this reversal readily translated into improvement of midshaft femoral diaphysis mechanical properties, which was evidenced by the increased stiffness and ultimate load determined by 4-point bending and by the considerably high correlation of cortical thickness to both stiffness and maximum force that cortical bone could withstand before fracture occurred. This finding is consistent with published correlation studies[46, 47] and previous papers where an OVX- or glucocorticoid-induced severe osteoporosis model treated with Scl-Ab was examined[48, 49].

The findings from this study extend our understanding of Scl-Ab as a potent therapeutic anabolic agent to counteract the severe bone loss condition associated with mechanical unloading and/or estrogen depletion[32], indicating that Scl-Ab is capable of preventing the extreme cortical and trabecular bone loss that develops during HLS and/or OVX. The evidence presented is believed to be of great clinical relevance as severe osteoporosis induced by long-term immobilization and estrogen deficiency is not uncommon in women, especially those who are over 50 years old, as they are also reported to be the most sedentary group in adult populations[50]. Although the extent to which trabecular bone deteriorated due to the combination of mechanical unloading and estrogen deficiency was remarkably greater than that seen in conditions such as long-term space travel, bed rest alone, or postmenopausal estrogen deficiency alone,[15] and possibly comparable to that of severe

osteoporosis developed after spinal cord injury, cortical bone did not suffer such severe bone thickness loss despite significant deterioration mechanical properties[51].

Our dynamic histomorphometry data showed a significant inhibition of the bone formation rate in the periosteum of the HLS and HLS + OVX groups after five weeks with Veh treatment, as well as a noticeable decrease of bone formation in the endosteum of HLS alone animals with Veh treatment as compared with the age-matched control. Regardless of the conditions that animals were subjected to (HLS alone, OVX alone or HLS + OVX), histomorphometry analyses indicate that five weeks of Scl-Ab administration resulted in a rapid and remarkable increase in cortical bone width, which is thought to be associated with robust bone formation at both the periosteum and endosteum. Similar results have been reported in studies of the effect of romosozumab (Scl-Ab) on bone mass and strength in OVX animals[35, 52]. Our study, however, is the first to report that Scl-Ab is capable of preserving cortical bone strength and structure by significantly improving bone formation indices in both the periosteum and endosteum. Taking this result and our previous study[32, 33] together, it suggests that 5 weeks of Scl-Ab treatment induces and sustains a global bone formation response on endocortical, periosteal, and trabecular surfaces. However, it was suggested by Stolina *et al.* that although this dynamic bone formation stimulation remained significant in the longer term, all surfaces had a decreased bone formation response at week 26[35]. The attenuation of bone formation after long-term Scl-Ab treatment was suggested to be due to the triggering of osteocyte-based negative feedback loops that are in place to prevent accumulation of an excessive amount of bone mass, since serum sclerostin level are positively correlated in general with naturally greater bone mass or gains of new bone mass in humans[53, 54].

Numerous studies have underlined the osteocyte's critical role as the major mechanosensor of bone, which it regulates by detecting mechanical signals and communicating with other cells in bone[55, 56]. Accumulating evidence has suggested that the osteocyte also plays an important role in endocrine regulation of mineral homeostasis, both locally through lacuna matrix resorption and through releasing factors that could affect distant organs[22, 57]. Usually, these osteocytes are dispersed throughout the mineralized cortical bone and are connected with one another through long dendritic processes that are highly sensitive for sensing mechanical forces[58]. The dendritic network also connects embedded bone cells with bone surface osteoblasts that regulate bone formation as well as resorptive osteoclast precursors, which reinforces its role as a major mechanosensor and mediator for mechanical forces and cellular processes in the bone[59–61]. Hence, it is conceivable that deformation of the cellular morphology and connections of osteocytes and the dendritic network may likely lead to the disruption of inter-osteocyte communication as well as communication between osteocytes and other cells in bone[35, 58, 62–65]. Our SEM analysis showed that HLS, OVX, and HLS + OVX lead to multiple morphological and structural changes in the osteocytes and dendrites in femur midshaft cortical bone, including reduced osteocyte numbers per unit area of cortical bone and reduced dendrite number per osteocyte. In addition, morphological changes in the osteocytes were also identified, where the oval-shaped osteocytes became thinner and longer. These results are in line with the fact that mechanical unloading may change the gene expression of osteocytes *in vivo* and thus affect osteocyte function and morphology,[62] primarily through sclerostin blocking the activation of the Wnt/ β-catenin

signaling pathway[18, 23]. Furthermore, estrogen depletion may also trigger a negative response from osteocytes since it is believed that estrogen regulates bone metabolism through crosstalk between Wnt/ β-catenin and estrogen receptor α (ERα) since ERα may be able to transport β-catenin into the osteocyte nucleus based on mechanical cues[66]. Estrogen deficiency and concurrent mechanical unloading may therefore involve multiple signaling pathways converging through β-catenin.

Interestingly, although HLS and/or OVX both lead to bone loss and structural changes, the cellular mechanisms might be divergent, as evidenced by our measurements of the osteocyte volume and the long axis and short axis ratio (LASAR) parameters under these conditions. The SEM analysis indicates that HLS alone is associated with a larger LASAR without an increase in osteocyte volume, which caused an osteocyte morphological shift from an oval-shaped cell body to a more spindle-shaped one, while in the OVX alone group, the oblong osteocyte is increased in volume, which helps to largely maintain its oval shape. This coincides with the notion that the mechanisms of bone loss caused by mechanical unloading and estrogen deficiency are different. It has been speculated that the elogation of osteocytes in the hindlimb suspension condition represents an adaptive response to mechanical unloading since it is evident that osteocytes can sense and respond to specific mechanical signals under different volumetric deformations that change the load-induced fluid flow. The deformation and change of shape could give rise to functional differences as that may have an impact on the transfer of stress information to osteocytes. Although further study is still required to fully characterize the relationship of osteocytes' morphological change and their functions, there is no doubt that the change is associated with osteoporosis since the sensing of and the sensitivity to strain and fluid flow inputs to the osteocyte are altered with variations in osteocyte morphology[67].

Scl-Ab treatment significantly decreases LASAR in the HLS alone and OVX alone groups such that it is lower in these two groups than the age-matched control, while Scl-Ab treatment in the HLS + OVX group only slightly decreased LASAR. Contrary to the seemingly more consistent change in LASAR across the groups, osteocyte volume change following Scl-Ab treatment is divergent, with the HLS group increasing while the OVX group decreases significantly and the HLS + OVX group remains stable compared to the respective controls. It seems that Scl-Ab tunes the volume of osteocytes towards the age-matched control level in the HLS and OVX groups while failing to do so in the HLS + OVX group, which indicates other cellular mechanisms also play roles in the osteocyte's response to HLS and/or OVX and the treatment with Scl-Ab. Our study, being the first to examine the effect of immobilization and concurrent estrogen deficiency on osteocytic network, morphology, and structure in the cortical bone of the femur midshaft, complements previous studies and further emphasizes the notion that osteoporosis developed under various conditions may share common cellular mechanisms. It also becomes clear that the consequences of osteoporosis, regardless of its etiology, are systemically evident across multiple anatomical sites and among different tissues, including femur cortical and trabecular bone at the midshaft or femoral head and alveolar bone[68]. At the same time, it was also observed that the bone matrix around osteocytes has a less dense woven appearance, with disorganized and poor mineralization, as compared with the age-matched control group. Similar deterioration has been documented in previous immobilization

studies[8, 64]. Schneider *et al.*[64] discovered that osteocyte morphology and the structure of cortical sheath of the femoral neck in osteoporotic and osteoarthritic patients are subject to similar degradation. Notably, in accord with the finding, Qin *et al.*[8] reported that severe bone loss following acute motor-complete spinal cord injury resulted in reduced osteocyte and dendrite numbers, poor bone matrix quality, and irregular mineral distribution.

Most remarkably, our study demonstrated that Scl-Ab administration could largely preserve the morphology and structure of osteocytes and maintain matrix integrity by abolishing the decrease in osteocyte density and dendrite number following mechanical unloading and concurrent estrogen deficiency. It is possible that following the improvement in osteocyte density as well as the osteocyte dendritic network, osteocyte functions such as mechanotransduction, mechanosensing, and secretion of major osteocyte proteins may resume and exert their promotional effects through a cascade of events on bone remodeling, with improved bone formation and inhibited bone resorption. It also suggests that Scl-Ab is capable of inhibiting sclerostin, one of the chemical signals associated with osteocytic deformation and dysfunction resulting from concurrent immobilization and estrogen depletion. The therapeutic effect of Scl-Ab on osteocyte morphology and structure through the inactivation of sclerostin is associated with a decreased level of sclerostin in the osteocytes' microenvironment, which supports the view that increased sclerostin concentration in the osteocyte microenvironment is sufficient to induce abnormal changes in osteocytic parameters[8, 62]. Overall, our study indicates the crucial effect of sclerostin on osteocytes and their role as the major orchestrator during the bone remodeling process.

In summary, we utilized a severe osteoporosis model incorporating both mechanical unloading and OVX to mimic one of the severest forms of bone loss experienced especially by elderly women. The 5-week study demonstrated severe midshaft cortical bone thinning and decreased bone formation at both endocortical and periosteal sites that ultimately translated into significantly compromised mechanical properties. We tried to understand the cellular mechanisms underlying these findings by associating the morphological and structural deterioration of osteocytes and their matrix with mechanical unloading and concurrent estrogen depletion. With short-term inhibition of sclerostin induced by administrating Scl-Ab, the deterioration in cortical bone thickness and mechanical properties were completely reversed due to robust bone formation observed at both the endocortical and periosteal surface. This efficacious intervention for severe bone loss in our model was linked with ability of Scl-Ab to restore osteocyte morphology, structure, and its microenvironment by neutralizing sclerostin and to normalize the bone remodeling process that involves both osteoblastogenesis and osteoclastogenesis, which were impaired after mechanical unloading and concomitant estrogen depletion. These results suggest that monoclonal sclerostin-neutralizing antibody preserves bone in severe osteoporotic conditions and represents a strong candidate for clinical applications and a promising new therapeutic approach for severe osteoporosis.

Acknowledgments

This work was kindly supported by the National Institute of Health (R01 AR52379 and R01 AR61821), the US Army Medical Research and Materiel Command, and by Amgen, Inc. The authors thank Amgen, Inc. for providing Scl-Ab. The authors would also like to thank all the members in the Orthopaedic Bioengineering Research Lab at

Stony Brook University and the labs in the Department of Material Science Engineering Department, particularly Dr. James Quinn for assistance in the SEM analysis, and Alyssa Tuthill for assistance in the animal experiments.

References

1. Zaidi M Skeletal remodeling in health and disease. Nat Med. 2007;13: 791–801. [PubMed: 17618270]
2. Mitchner NA, Harris ST. Current and emerging therapies for osteoporosis. J Fam Pract. 2009;58: S45–49. [PubMed: 19825319]
3. Sunyecz JA. The use of calcium and vitamin D in the management of osteoporosis. Ther Clin Risk Manag. 2008;4: 827–836. [PubMed: 19209265]
4. Cauley JA. Public Health Impact of Osteoporosis. J Gerontol A Biol Sci Med Sci. 2013.
5. Becker DJ, Kilgore ML, Morrisey MA. The societal burden of osteoporosis. Curr Rheumatol Rep. 2010;12: 186–191. [PubMed: 20425518]
6. Burge R, Dawson-Hughes B, Solomon DH, Wong JB, King A, Tosteson A. Incidence and Economic Burden of Osteoporosis-Related Fractures in the United States, 2005–2025. Journal of Bone and Mineral Research. 2007;22: 465–475. [PubMed: 17144789]
7. Das S, Crockett JC. Osteoporosis - a current view of pharmacological prevention and treatment. Drug Des Devel Ther. 2013;7: 435–448.
8. Qin W, Li X, Peng Y, et al. Sclerostin antibody preserves the morphology and structure of osteocytes and blocks the severe skeletal deterioration after motor-complete spinal cord injury in rats. J Bone Miner Res. 2015;30: 1994–2004. [PubMed: 25974843]
9. Crockett JC, Mellis DJ, Scott DI, Helfrich MH. New knowledge on critical osteoclast formation and activation pathways from study of rare genetic diseases of osteoclasts: focus on the RANK/RANKL axis. Osteoporosis International. 2011;22: 1–20.
10. Phan TC, Xu J, Zheng MH. Interaction between osteoblast and osteoclast: impact in bone disease. Histol Histopathol. 2004;19: 1325–1344. [PubMed: 15375775]
11. Almeida M, Laurent MR, Dubois V, et al. Estrogens and Androgens in Skeletal Physiology and Pathophysiology. Physiol Rev. 2017;97: 135–187. [PubMed: 27807202]
12. Vico L, Chappard D, Alexandre C, et al. Effects of a 120 day period of bed-rest on bone mass and bone cell activities in man: attempts at countermeasure. Bone Miner. 1987;2: 383–394. [PubMed: 3146359]
13. Gaudio A, Pennisi P, Bratengeier C, et al. Increased sclerostin serum levels associated with bone formation and resorption markers in patients with immobilization-induced bone loss. J Clin Endocrinol Metab. 2010;95: 2248–2253. [PubMed: 20305005]
14. Fiore CE, Pennisi P, Ciffo F, Scebba C, Amico A, Di Fazzio S. Immobilization-dependent bone collagen breakdown appears to increase with time: evidence for a lack of new bone equilibrium in response to reduced load during prolonged bed rest. Horm Metab Res. 1999;31: 31–36. [PubMed: 10077347]
15. Qin W, Bauman WA, Cardozo C. Bone and muscle loss after spinal cord injury: organ interactions. Ann N Y Acad Sci. 2010;1211: 66–84. [PubMed: 21062296]
16. Tou JC, Foley A, Yuan YV, Arnaud S, Wade CE, Brown M. The effect of ovariectomy combined with hindlimb unloading and reloading on the long bones of mature Sprague-Dawley rats. Menopause. 2008;15: 494–502. [PubMed: 18030174]
17. Kim BJ, Bae SJ, Lee SY, et al. TNF-alpha mediates the stimulation of sclerostin expression in an estrogen-deficient condition. Biochem Biophys Res Commun. 2012;424: 170–175. [PubMed: 22735261]
18. Li X, Zhang Y, Kang H, et al. Sclerostin binds to LRP5/6 and antagonizes canonical Wnt signaling. J Biol Chem. 2005;280: 19883–19887. [PubMed: 15778503]
19. Li X, Ominsky MS, Warmington KS, et al. Sclerostin antibody treatment increases bone formation, bone mass, and bone strength in a rat model of postmenopausal osteoporosis. J Bone Miner Res. 2009;24: 578–588. [PubMed: 19049336]
20. Winkler DG, Sutherland MK, Geoghegan JC, et al. Osteocyte control of bone formation via sclerostin, a novel BMP antagonist. EMBO J. 2003;22: 6267–6276. [PubMed: 14633986]

21. Rossini M, Gatti D, Adami S. Involvement of WNT/beta-catenin Signaling in the Treatment of Osteoporosis. Calcif Tissue Int. 2013;93: 121–132. [PubMed: 23748710]
22. Poole KE, van Bezooijen RL, Loveridge N, et al. Sclerostin is a delayed secreted product of osteocytes that inhibits bone formation. FASEB J. 2005;19: 1842–1844. [PubMed: 16123173]
23. van Bezooijen RL, ten Dijke P, Papapoulos SE, Lowik CW. SOST/sclerostin, an osteocyte-derived negative regulator of bone formation. Cytokine Growth Factor Rev. 2005;16: 319–327. [PubMed: 15869900]
24. Bonewald LF, Johnson ML. Osteocytes, mechanosensing and Wnt signaling. Bone. 2008;42: 606–615. [PubMed: 18280232]
25. Ke HZ, Richards WG, Li X, Ominsky MS. Sclerostin and Dickkopf-1 as therapeutic targets in bone diseases. Endocr Rev. 2012;33: 747–783. [PubMed: 22723594]
26. Tella SH, Gallagher JC. Prevention and treatment of postmenopausal osteoporosis. J Steroid Biochem Mol Biol. 2014;142: 155–170. [PubMed: 24176761]
27. Lin C, Jiang X, Dai Z, et al. Sclerostin mediates bone response to mechanical unloading through antagonizing Wnt/beta-catenin signaling. J Bone Miner Res. 2009;24: 1651–1661. [PubMed: 19419300]
28. Robling AG, Niziolek PJ, Baldridge LA, et al. Mechanical stimulation of bone in vivo reduces osteocyte expression of Sost/sclerostin. J Biol Chem. 2008;283: 5866–5875. [PubMed: 18089564]
29. Mirza FS, Padhi ID, Raisz LG, Lorenzo JA. Serum Sclerostin Levels Negatively Correlate with Parathyroid Hormone Levels and Free Estrogen Index in Postmenopausal Women. J Clin Endocrinol Metab. 2010;95: 1991–1997. [PubMed: 20156921]
30. Gallagher JC, Tella SH. Prevention and treatment of postmenopausal osteoporosis. J Steroid Biochem Mol Biol. 2014;142: 155–170. [PubMed: 24176761]
31. Kohli SS, Kohli VS. Role of RANKL–RANK/osteoprotegerin molecular complex in bone remodeling and its immunopathologic implications. Indian Journal of Endocrinology and Metabolism. 2011;15: 175–181. [PubMed: 21897893]
32. Zhang D, Hu M, Chu T, et al. Sclerostin antibody prevented progressive bone loss in combined ovariectomized and concurrent functional disuse. Bone. 2016;87: 161–168. [PubMed: 26868528]
33. Zhang D, Hu M, Chu T, et al. Erratum to Sclerostin antibody prevented progressive bone loss in combined ovariectomized and concurrent functional disuse [Bone 87 (2016) 161–168]. Bone. 2016;89: 86. [PubMed: 27262889]
34. Lam H, Hu M, Qin YX. Alteration of contraction-to-rest ratio to optimize trabecular bone adaptation induced by dynamic muscle stimulation. Bone. 2011;48: 399–405. [PubMed: 20850577]
35. Stolina M, Dwyer D, Niu QT, et al. Temporal changes in systemic and local expression of bone turnover markers during six months of sclerostin antibody administration to ovariectomized rats. Bone. 2014;67: 305–313. [PubMed: 25093263]
36. Chen H, Xu X, Liu M, et al. Sclerostin antibody treatment causes greater alveolar crest height and bone mass in an ovariectomized rat model of localized periodontitis. Bone. 2015;76: 141–148. [PubMed: 25868799]
37. Martin DM, Hallsworth AS, Buckley T. A method for the study of internal spaces in hard tissue matrices by SEM, with special reference to dentine. J Microsc. 1978;112: 345–352. [PubMed: 347084]
38. Lu Y, Xie Y, Zhang S, Dusevich V, Bonewald LF, Feng JQ. DMP1-targeted Cre expression in odontoblasts and osteocytes. J Dent Res. 2007;86: 320–325. [PubMed: 17384025]
39. Weinreb M, Patael H, Preisler O, Ben-Shemen S. Short-term healing kinetics of cortical and cancellous bone osteopenia induced by unloading during the reloading period in young rats. Virchows Arch. 1997;431: 449–452. [PubMed: 9428933]
40. Bikle DD, Halloran BP. The response of bone to unloading. J Bone Miner Metab. 1999;17: 233–244. [PubMed: 10575587]
41. Shahnazari M, Wronski T, Chu V, et al. Early response of bone marrow osteoprogenitors to skeletal unloading and sclerostin antibody. Calcif Tissue Int. 2012;91: 50–58. [PubMed: 22644321]
42. Raisz LG, Prestwood KM. Epidemiology and pathogenesis of osteoporosis. Clin Cornerstone. 2000;2: 1–10.

43. Tian X, Jee WS, Li X, Paszty C, Ke HZ. Sclerostin antibody increases bone mass by stimulating bone formation and inhibiting bone resorption in a hindlimb-immobilization rat model. Bone. 2011;48: 197–201. [PubMed: 20850580]
44. Spatz JM, Ellman R, Cloutier AM, et al. Sclerostin antibody inhibits skeletal deterioration due to reduced mechanical loading. J Bone Miner Res. 2013;28: 865–874. [PubMed: 23109229]
45. Spatz JM, Fields EE, Yu EW, et al. Serum sclerostin increases in healthy adult men during bed rest. J Clin Endocrinol Metab. 2012;97: E1736–1740. [PubMed: 22767636]
46. Bagi CM, Hanson N, Andresen C, et al. The use of micro-CT to evaluate cortical bone geometry and strength in nude rats: correlation with mechanical testing, pQCT and DXA. Bone. 2006;38: 136–144. [PubMed: 16301011]
47. Ferretti JL, Capozza RF, Mondelo N, Zanchetta JR. Interrelationships between densitometric, geometric, and mechanical properties of rat femora: inferences concerning mechanical regulation of bone modeling. J Bone Miner Res. 1993;8: 1389–1396. [PubMed: 8266830]
48. Yao W, Dai W, Jiang L, et al. Sclerostin-antibody treatment of glucocorticoid-induced osteoporosis maintained bone mass and strength. Osteoporosis International. 2016;27: 283–294. [PubMed: 26384674]
49. Virdi AS, Irish J, Sena K, et al. Sclerostin Antibody Treatment Improves Implant Fixation in a Model of Severe Osteoporosis. The Journal of Bone & Joint Surgery. 2015;97: 133–140. [PubMed: 25609440]
50. King AC, Rejeski WJ, Buchner DM. Physical activity interventions targeting older adults. A critical review and recommendations. Am J Prev Med. 1998;15: 316–333. [PubMed: 9838975]
51. Qin Y-X, Liu J, Zhang D, Li X. Acceleration of critical bone defect healing by guided low-intensity ultrasound in a rat tibial model. The Journal of the Acoustical Society of America. 2016;140: 3191–3191.
52. Ominsky MS, Boyd SK, Varela A, et al. Romosozumab Improves Bone Mass and Strength While Maintaining Bone Quality in Ovariectomized Cynomolgus Monkeys. J Bone Miner Res. 2016.
53. Gatti D, Viapiana O, Idolazzi L, Fracassi E, Rossini M, Adami S. The Waning of Teriparatide Effect on Bone Formation Markers in Postmenopausal Osteoporosis Is Associated with Increasing Serum Levels of DKK1. The Journal of Clinical Endocrinology & Metabolism. 2011;96: 1555–1559. [PubMed: 21367927]
54. Gatti D, Viapiana O, Adami S, Idolazzi L, Fracassi E, Rossini M. Bisphosphonate treatment of postmenopausal osteoporosis is associated with a dose dependent increase in serum sclerostin. Bone. 2012;50: 739–742. [PubMed: 22178539]
55. Shahar R, Dean MN. The enigmas of bone without osteocytes. BoneKEy Rep. 2013;2.
56. Abstracts of the 28th Annual Meeting of the American Society for Bone and Mineral Research, 9 15–19, 2006, Philadelphia, Pennsylvania, USA. J Bone Miner Res. 2006;21 Suppl 1: S2–460. [PubMed: 17054317]
57. Cardoso L, Herman BC, Verborgt O, Laudier D, Majeska RJ, Schaffler MB. Osteocyte apoptosis controls activation of intracortical resorption in response to bone fatigue. J Bone Miner Res. 2009;24: 597–605. [PubMed: 19049324]
58. Bonewald LF, Johnson ML. Osteocytes, Mechanosensing and Wnt Signaling. Bone. 2008;42: 606–615. [PubMed: 18280232]
59. Zhao S, Zhang YK, Harris S, Ahuja SS, Bonewald LF. MLO-Y4 osteocyte-like cells support osteoclast formation and activation. J Bone Miner Res. 2002;17: 2068–2079. [PubMed: 12412815]
60. Kamioka H, Honjo T, Takano-Yamamoto T. A three-dimensional distribution of osteocyte processes revealed by the combination of confocal laser scanning microscopy and differential interference contrast microscopy. Bone. 2001;28: 145–149. [PubMed: 11182371]
61. Baylink D, Sipe J, Wergedal J, Whittemore OJ. Vitamin D-enhanced osteocytic and osteoclastic bone resorption. Am J Physiol. 1973;224: 1345–1357. [PubMed: 4712149]
62. Bonewald LF. The amazing osteocyte. J Bone Miner Res. 2011;26: 229–238. [PubMed: 21254230]
63. Bacabac RG, Mizuno D, Schmidt CF, et al. Round versus flat: Bone cell morphology, elasticity, and mechanosensing. Journal of Biomechanics. 2008;41: 1590–1598. [PubMed: 18402963]
64. Schneider P, Meier M, Wepf R, Müller R. Towards quantitative 3D imaging of the osteocyte lacuno-canalicular network. Bone. 2010;47: 848–858. [PubMed: 20691297]

65. Burra S, Nicolella DP, Francis WL, et al. Dendritic processes of osteocytes are mechanotransducers that induce the opening of hemichannels. Proceedings of the National Academy of Sciences. 2010;107: 13648–13653.

66. Zaman G, Jessop HL, Muzylak M, et al. Osteocytes use estrogen receptor alpha to respond to strain but their ERalpha content is regulated by estrogen. J Bone Miner Res. 2006;21: 1297–1306. [PubMed: 16869728]

67. van Oers RF, Wang H, Bacabac RG. Osteocyte shape and mechanical loading. Curr Osteoporos Rep. 2015;13: 61–66. [PubMed: 25663071]

68. Rawlinson SC, Boyde A, Davis GR, Howell PG, Hughes FJ, Kingsmill VJ. Ovariectomy vs. hypofunction: their effects on rat mandibular bone. J Dent Res. 2009;88: 615–620. [PubMed: 19641148]

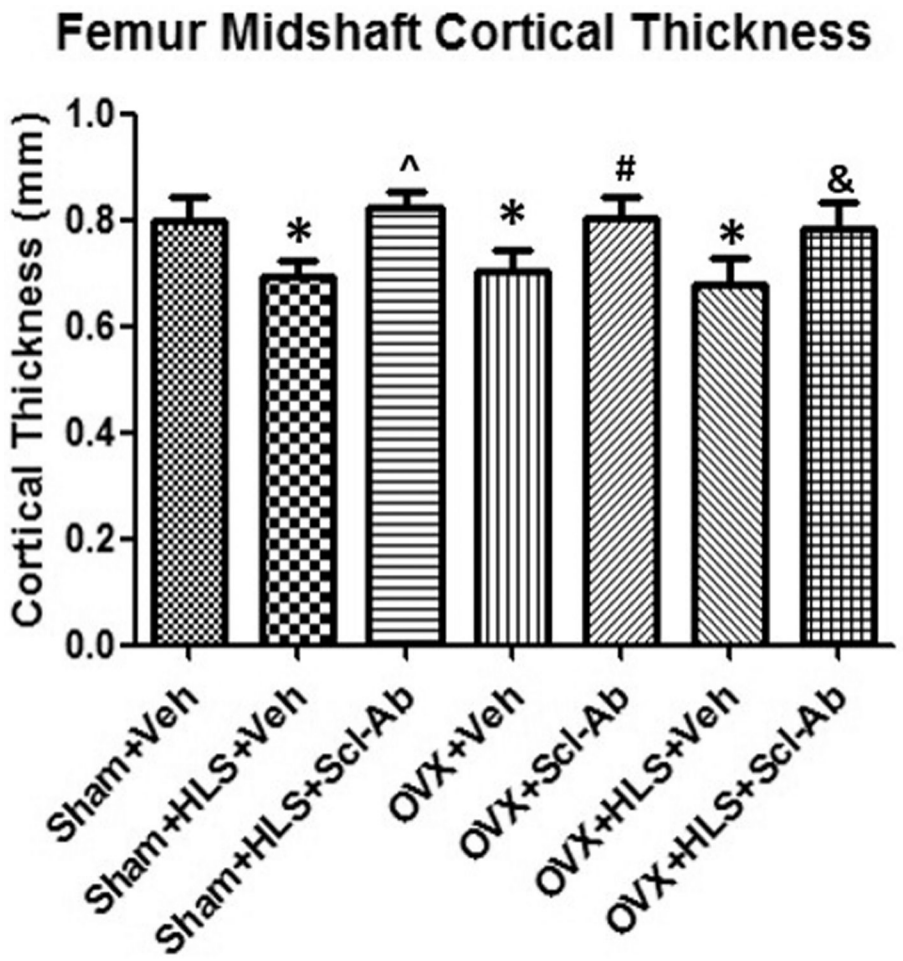

Figure 1.

Graph of the mean ± SD values for μCT cortical thickness (Ct.Th.) at the femur midshaft. $^{*}P < 0.05$ vs. Sham + Veh; $^{\wedge}P < 0.05$ vs. Sham + HLS + Veh; $^{\#}P < 0.05$ vs. OVX + Veh; $^{\&}P < 0.05$ vs. OVX + HLS + Veh.

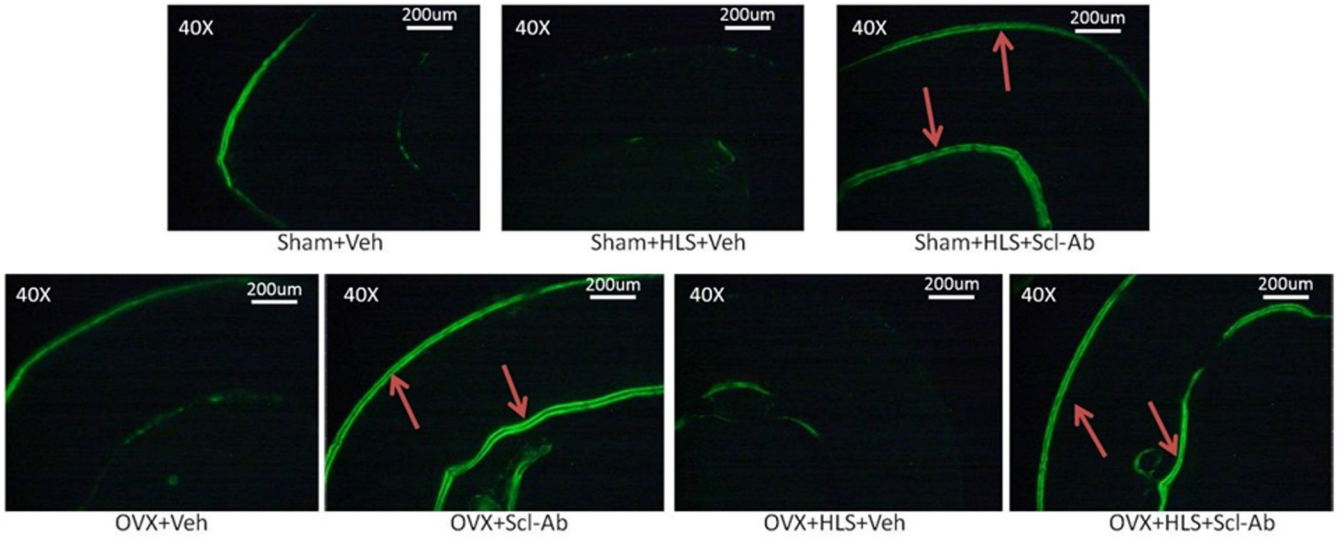

Figure 2.

Representative images of calcein-labeled cortical bone at the femoral midshaft. Red arrows indicate double labels observed at the endosteum and periosteum surface.

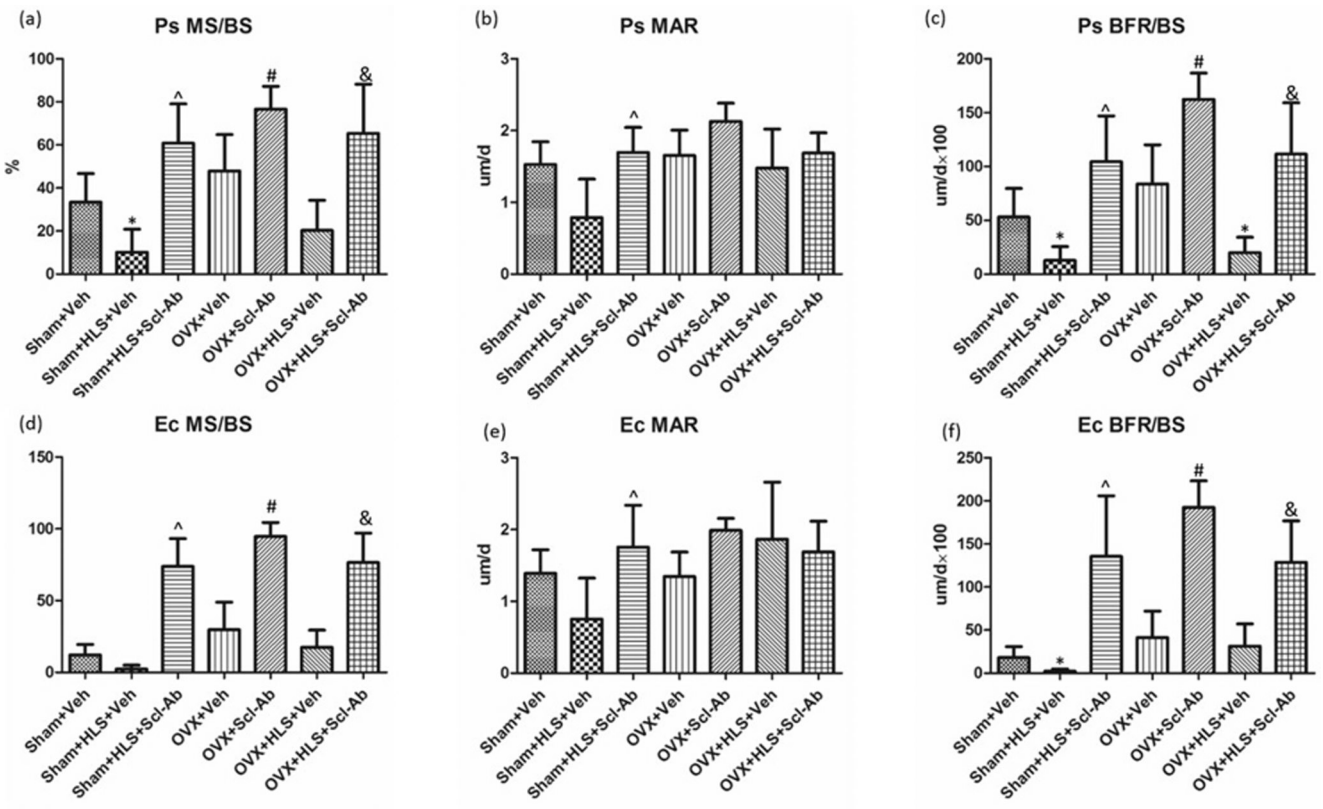

Figure 3.

Graphs of the mean ± SD values for the histomorphometric parameters Ps. MS/BS (A), Ps. MAR (B), Ps. BFR/BS (C), Ec. MS/BS (D), Ec. MAR (E), and Ec. BFR/BS (F). $^{*}P < 0.05$ vs. Sham + Veh; $^{\wedge}P < 0.05$ vs. Sham + HLS + Veh; $^{\#}P < 0.05$ vs. OVX + Veh; $^{\&}P < 0.05$ vs. OVX + HLS + Veh.

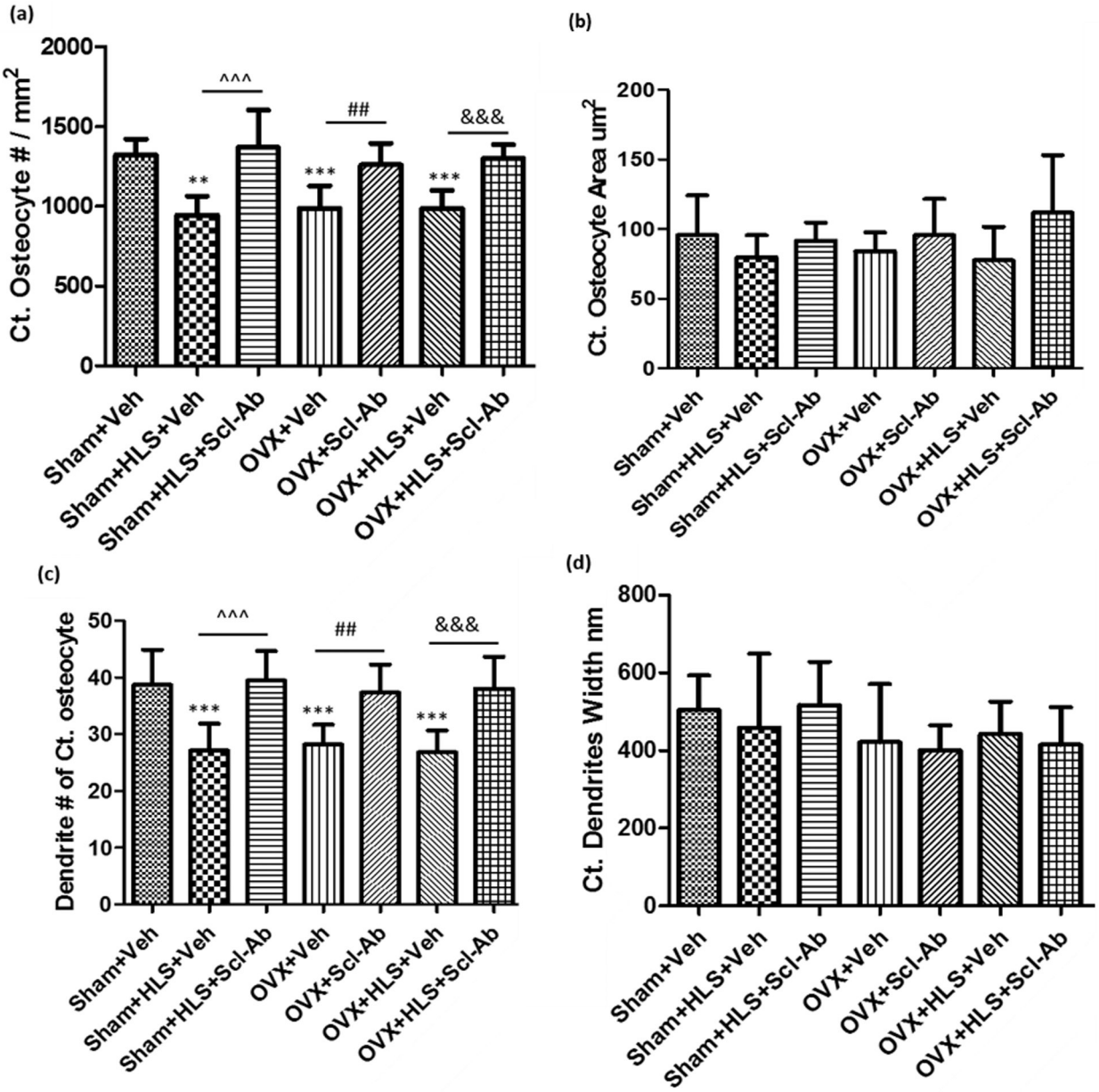

Figure 4.

(A) Graph of the mean ± SD values for cortical osteocyte number per tissue area (Ct. Osteocyte #/mm^2). (B) Graph of the mean ± SD values for cortical osteocyte area (μm^2). (C) Graph of the mean ± SD values of dendrite # of cortical osteocyte. (D) Graph of the mean ± SD values of cortical dendrite width (nm). $^{**}P < 0.01$, $^{***}P < 0.001$ versus Sham + Veh; $^{\wedge\wedge\wedge}P < 0.001$, $^{\#\#}P < 0.01$ and $^{\&\&\&}P < 0.001$ versus the indicated group.

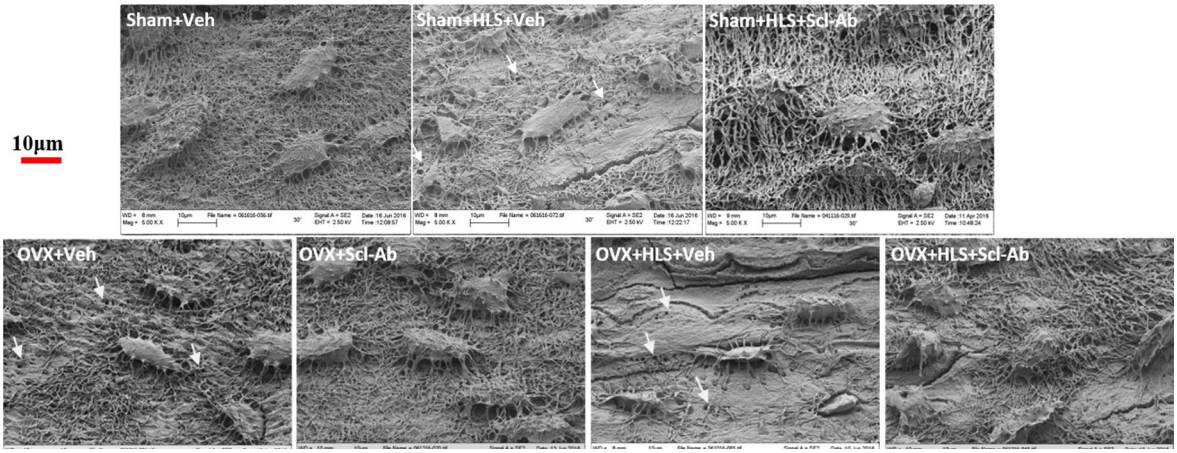

Figure 5.

Representative 5000 × SEM images showing osteocyte morphological and structural changes following Veh or Scl-Ab treatment of HLS, OVX, and HLS + OVX animals. White arrows indicate areas of poor mineralization of the bone matrix.

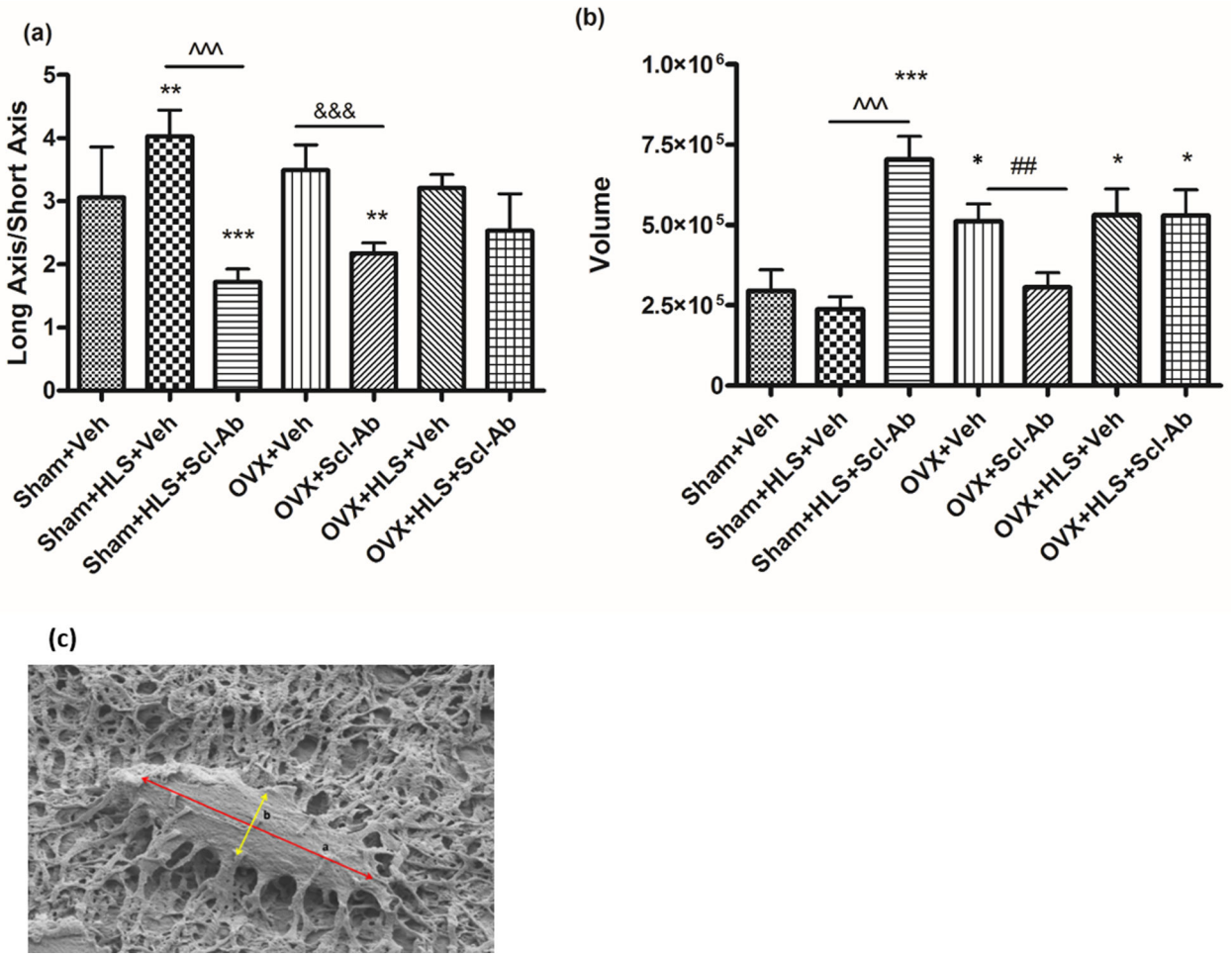

Figure 6.

(A) Graph of the mean ± SD values for the ratio of the long axis and short axis of osteocytes. (** $P < 0.01$ vs. Sham + Veh; *** $P < 0.001$ vs. Sham + Veh; $^{\wedge\wedge\wedge}P < 0.001$ and $^{\&\&\&}P < 0.001$ vs. the indicated group). (B) Graph of the mean ± SD values for the volume of osteocytes. (** $P < 0.01$ vs. Sham+ Veh; *** $P < 0.001$ vs. Sham+Veh; $^{\wedge\wedge\wedge}P < 0.001$, $^{\&\&\&}P < 0.001$ and $^{\#\#}P < 0.05$ vs. the indicated group). c) Osteocyte with long axis (a) and short axis (b).

Table 1.

Correlations between μCT-measured Ct.Th. and stiffness and ultimate load

	Cortical thickness (mm)	Stiffness (kN/mm)	Ultimate load (N)
Sham + Veh	0.8005	1.1532	292.9
Sham + HLS + Veh	0.6910	0.8879	271.1
Sham + HLS + Scl-Ab	0.8067	1.1632	365.9
OVX + Veh	0.7055	0.9628	251.2
OVX + Scl-Ab	0.8030	1.2708	392.6
OVX + HLS + Veh	0.6791	0.8187	239.4
OVX + HLS + Scl-Ab	0.7820	1.2854	313.4
Correlation (R^2)		**0.8625**	**0.7081**